**Edelweiss Applied Science and Technology**
*ISSN: 2576-8484*
*Vol. 9, No. 11, 429-447*
*2025*
*Publisher: Learning Gate*
*DOI: 10.55214/2576-8484.v9i11.10879*
*© 2025 by the authors; licensee Learning Gate*

# Adsorption of hydrogen sulfide on synthetic and carbon adsorbents: Isotherms and mechanism

Oybek Ergashev[1], Khayot Bakhronov[2*], Mirzokhid Kokhkharov[3], Jumaboeva Zebo[4], Muratali Bazarbaev[5], Amirkhon Sultonov[6], Surayyo Sobirjonova[7], Ziyoda Juraeva[8], Marufjon Asfandiyorov[9], Dildora Gaybullayeva[10]
[1,3,6,7]Namangan State Technical University, Namangan, Uzbekistan; okergashev711@gmail.com (O.E) mirzo199008@mail.ru (M.K) amirxonsultonov34@gmail.com (A.S) sobirjonovasurayyo59@gmail.com (S.S).
[2,4,9]Tashkent University of Information Technologies named after Muhammad al-Khwarizmi, Tashkent, Uzbekistan; baxronov@mail.ru (K.B.) zjumaboeva19@gmail.com (J.Z) masfandiyorov@tuit.uz (M.A).
[5,8]Tashkent Medical Academy, Tashkent, Uzbekistan; m.bazarbaev@tma.uz (M.B) ziyodajurayeva1994@gmail.com (Z.J).
[10]The Branch of the Russian State University of Oil and Gas (National Research University) named after I.M. Gubkin in Tashkent, Uzbekistan; xurramovadildora0@gmail.com (D.G).

**Abstract:** The adsorption of hydrogen sulfide ($H_2S$) was studied using the adsorption calorimetric method at a constant temperature of 303 K. The objects of study were CaA-type zeolites with different cationic compositions and a carbon adsorbent obtained by microwave activation of Paulownia tomentosa bark. The obtained adsorption isotherms were processed using the Dubinin–Radushkevich equation, which made it possible to determine the adsorption capacity, characteristic energy, and the nature of the interaction between $H_2S$ molecules and the active surface sites. The isotherm expressed in the three-term form of the Volume Micropore Occupation Theory (VMOT) equation showed complete agreement with the experimental data. Based on these equations, the adsorption isotherm was calculated up to the saturation vapor pressure of $H_2S$. Calorimetric results indicated a moderate exothermic effect typical of predominantly physical adsorption accompanied by weak chemisorption on certain active centers. Differences in the sorption behavior of zeolites and the carbon adsorbent were attributed to variations in pore structure, surface polarity, and the concentration of active sites. The obtained results refine the thermodynamic characteristics of the $H_2S$-solid adsorbent system and can be applied to the development of efficient technologies for the purification of natural and industrial gases from hydrogen sulfide.

***Keywords:*** *Adsorption mechanism, Adsorption, Hydrogen sulfide, Isotherm, Tomentosa, Zeolite.*

## 1. Introduction

Hydrogen sulfide ($H_2S$) is a colorless gas with a characteristic "rotten egg" odor, exhibiting high toxicity and corrosive activity. Its presence in natural, petroleum, and biogases is one of the major challenges faced by the chemical and energy industries. Concentrations of $H_2S$ above 10-20 ppm already pose a serious threat to human health, while exposure to 300 ppm may cause acute damage to the respiratory system and neural tissues [1]. In addition to its toxicological impact, $H_2S$ induces severe corrosion of metal pipelines and process equipment, significantly reducing their service life [2].

The primary sources of hydrogen sulfide include natural and associated petroleum gases, biogas, products of thermal decomposition of sulfur-containing organic compounds, and exhaust gases from petrochemical facilities. The $H_2S$ content in natural gases from various deposits can range from trace amounts to 10-15 vol.% [3].

The purification of gas streams from hydrogen sulfide is a key technological task aimed at improving energy resource quality and reducing harmful emissions. The most widely used methods are

*© 2025 by the authors; licensee Learning Gate*
**History:** Received: 27 August 2025; Revised: 9 October 2025; Accepted: 14 October2025; Published: 5 November 2025
* Correspondence: baxronov@mail.ru

chemical absorption in aqueous solutions of monoethanolamine (MEA), diethanolamine (DEA), methyldiethanolamine (MDEA), and alkaline solutions [4]. However, these methods require high energy consumption and complex sorbent regeneration procedures. In recent years, physico-chemical adsorption methods have been actively developed, providing high efficiency with lower operational costs [5].

Carbon-based adsorbents are among the most versatile and efficient materials for removing gaseous impurities, including $H_2S$. Due to their well-developed microporous structure, large specific surface area (500-1500 $m^2/g$), and chemical stability, activated carbons are widely employed in gas purification and catalysis processes [6]. The adsorption mechanism of hydrogen sulfide on carbon materials involves both physical and chemical interactions. Physical adsorption predominates in micropores (<2 nm), where $H_2S$ condensation occurs under the influence of the pore surface potential field, with an adsorption heat of 20–30 kJ/mol [7]. Chemical adsorption occurs on alkaline surface sites formed by the modification of carbon with compounds such as NaOH, $K_2CO_3$, ZnO, CuO, and others [8].

A promising direction is the production of biogenic carbons derived from plant-based raw materials, such as the bark of Paulownia tomentosa, coconut shells, olive pits, and others. Microwave activation of such precursors promotes the development of a highly microporous structure and increases the sorption capacity for $H_2S$ by 1.5-2 times compared to thermally activated counterparts [9]. In addition, carbon adsorbents exhibit excellent regeneration performance the recovery of sorption activity after thermovacuum desorption reaches 90–95%. This makes them economically advantageous for multi-cycle operation in natural gas and biogas purification systems.

Despite the high efficiency of carbon adsorbents, there is no structural or chemical relationship between them and synthetic zeolites, as these materials belong to different classes of solid porous substances. Carbon adsorbents are amorphous or partially graphitized structures dominated by micropores and characterized by a high specific surface area, where $H_2S$ adsorption occurs predominantly through physical mechanisms.

Zeolites, on the other hand, are crystalline aluminosilicates with a well-defined system of pores and ionic centers, where adsorption is governed by electrostatic interactions and cation exchange processes. Unlike carbons, zeolites lack π-electron systems capable of engaging in dispersion interactions with $H_2S$, and therefore exhibit a different type of sorption activity. Consequently, differences in the nature of active sites and pore structures preclude a direct correlation between the sorption characteristics of carbon and zeolite adsorbents. Nevertheless, their combination in the form of composite materials allows for the integration of the advantages of both systems high sorption capacity of carbon and selectivity of zeolites.

Synthetic zeolites are crystalline aluminosilicates characterized by a regular microporous framework and high ion-exchange capacity. Zeolite type A (LTA structure) has the chemical formula $Na_{12}[(AlO_2)_{12}(SiO_2)_{12}]\cdot 27H_2O$ and consists of cuboctahedral α- and β-cavities interconnected by eight-membered oxygen rings with an effective pore opening of approximately 0.41 nm [10]. Synthetic zeolite A (LTA, Linde Type A) is one of the most extensively studied and industrially utilized aluminosilicate adsorbents due to its unique combination of properties: highly ordered microporosity, pronounced ion-exchange ability, and strong selectivity toward water molecules and certain gases.

The LTA framework represents a three-dimensional network of ($SiO_4/AlO_4$) tetrahedra with a minimal Si/Al ratio of approximately 1. This low ratio results in a high density of negative framework charge and, consequently, a high concentration of compensating cations ($Na^+$, $K^+$, $Ca^{2+}$, etc.) located within the channels and cavities [11].

The conventional synthesis route for LTA involves hydrothermal crystallization in an alkaline medium using silicon and aluminum sources (typically $NaAlO_2$ and $Na_2SiO_3$ solutions), followed by crystallization at 60-100°C. The composition parameters and synthesis conditions determine the crystallite size, defect density, and cation distribution within the framework. Comprehensive reviews by Cundy and Cox [11] summarize the historical and mechanistic aspects of zeolite framework self-assembly, while more recent studies address sustainable "green" synthesis routes (e.g., from

*Edelweiss Applied Science and Technology*
*ISSN: 2576-8484*
*Vol. 9, No. 11: 429-447, 2025*
*DOI: 10.55214/2576-8484.v9i11.10879*
*© 2025 by the authors; licensee Learning Gate*

kaolinite/metakaolin) and process scale-up. Parallel research focuses on the development of binderless LTA materials ("binderless 4A") that offer improved mechanical integrity and adsorption efficiency [12].

The LTA framework consists of α-cages (supercages) with a diameter of approximately 11.4 Å, connected through "windows" formed by eight-membered oxygen rings. The effective aperture size of these windows depends on the type and position of the compensating cations. In the sodium form (Na-A, "4A"), the pore opening is about 4 Å; substitution of $Na^+$ with $K^+$ ("3A") reduces the opening to approximately 3 Å, whereas partial exchange with $Ca^{2+}$ ("5A") expands it to about 5 Å due to changes in the local cation coordination environment. This fine-tuning of the pore entrance forms the basis of classical molecular sieve separations according to kinetic diameter.

Due to its low Si/Al ratio and high anionic charge density, LTA zeolite is highly susceptible to ion exchange. The $Na^+ \rightarrow K^+$ exchange yields zeolite 3A, which is selective toward water and methanol while excluding larger molecules. The $Na^+ \rightarrow Ca^{2+}$ exchange results in zeolite 5A, which is effective for separating n-/i-paraffins and removing gas impurities with larger kinetic diameters. Control over the distribution of cations within α-cages and eight-membered rings allows for precise adjustment of both the pore size and the electrostatic field strength of active sites, which determine the adsorption enthalpy of polar molecules [13].

Substitution of sodium cations with calcium (CaA) decreases the electrostatic potential within the channels and increases the polarizability of the surface, thereby enhancing the adsorption properties of the zeolite toward polar molecules, including $H_2S$ [14]. According to Corma [14] the adsorption energy of $H_2S$ on CaA zeolite reaches 35–45 kJ/mol, indicating a mixed physico-chemical adsorption mechanism.

In addition, CaA zeolites possess pronounced catalytic properties arising from the acid–base activity of the aluminosilicate framework. They are effectively employed in isomerization, dehydration, hydrocracking, and hydrocarbon purification processes. The high thermal and mechanical stability of zeolites enables their multiple regeneration and reuse in high-temperature operations. The combined use of zeolites and carbon materials in composite adsorbents allows the integration of the microporous structure of zeolites with the high capacity of carbon. Such hybrid systems demonstrate enhanced sorption activity and thermal resistance during the purification of $H_2S$-containing gas streams [15].

Thus, analysis of the literature indicates that adsorption-based gas purification methods represent the most promising approach. The greatest interest lies in carbon and zeolitic adsorbents, which possess well-developed microporosity and tunable surface properties. While activated carbons provide high capacity due to their textural characteristics, CaA-type zeolites exhibit selectivity and stability derived from their ionic framework nature.

Based on the literature review, it is evident that carbon adsorbents derived from local plant biomass—particularly from bark, wood, and roots of various tree species—and activated by different methods vary significantly in their sorption and energetic characteristics. These differences depend both on the type of precursor material and on the activation method, as repeatedly noted by researchers. However, the literature lacks sufficient data on the sorption properties of activated carbon adsorbents derived from Paulownia tomentosa wood, as well as on CaA-type zeolites with respect to adsorbates of different physico-chemical natures, including hydrogen sulfide. The study of such adsorbents is therefore of current relevance, as the results can provide a basis for their application as efficient sorbents in various industrial technological processes.

It is well known that LTA zeolites exist in several forms, including NaA, CaA, and KA. The thermodynamic properties and adsorption mechanisms of polar, non-polar, and quadrupole molecules on NaA and CaA zeolites have been thoroughly studied [16-19]. Although the adsorption characteristics of various molecules with different sizes and physicochemical properties, including sulfur-containing compounds, on CaA zeolite have been investigated using X-ray and spectroscopic methods, there is still

*Edelweiss Applied Science and Technology*
*ISSN: 2576-8484*
*Vol. 9, No. 11: 429-447, 2025*
*DOI: 10.55214/2576-8484.v9i11.10879*
*© 2025 by the authors; licensee Learning Gate*

a lack of scientific research focused on the fundamental thermodynamic characteristics of these systems [20-23].

Calorimetric and isothermal studies conducted at 303 K provide fundamental insights into the mechanism of $H_2S$ sorption and the energetics of its interaction with active surface sites. These data form the basis for the development of new, highly efficient materials for the purification of natural and process gases, as well as for the construction of sorption equilibrium models based on the theory of volume filling of micropores (VMOT).

## 2. Testing Methods

For the measurement of adsorption isotherms, an experimental setup was employed that consisted of a universal high-vacuum adsorption unit connected to a Tian-Calvet-type differential heat-conducting microcalorimeter (model DAC-1-1A). The system is characterized by high precision, stability of readings, and exceptional sensitivity. Calibration of the instrument allows for the detection of thermal effects as low as approximately 0.2 μW, ensuring the reliability and reproducibility of data even during prolonged measurements. Due to its high sensitivity, the calorimeter can record thermal effects of processes lasting virtually unlimited durations and enables the study of the thermokinetics of adsorption systems, which is of great significance for elucidating the mechanism of interaction.

Structurally, the calorimeter is not a strictly adiabatic device: despite the presence of insulating shells, the heat released is partially transferred from the experimental chamber to a massive metallic block that serves as a thermal reservoir. The temperature within the calorimetric chamber changes only slightly; however, the instrument cannot be regarded as fully isothermal - the minimal temperature fluctuations it detects form the basis of the measurements and provide information on the direction of heat flow.

The adsorption-calorimetric method employed in this work ensures the acquisition of highly accurate molar thermodynamic characteristics and enables a detailed investigation of the adsorption processes occurring on the surface of adsorbents and catalysts. Measurement of isotherms and dosing of the adsorbate were carried out using a universal high-vacuum system that allows the introduction of the adsorbate in either gaseous or liquid–vapor form. The equilibrium pressure was determined with a BARATRON B-627 membrane gauge, noted for its high sensitivity and stability.

The operating principle and design features of the adsorption–calorimetric complex used in the present study are described in detail in the works of the authors [24-30].

## 3. Results and Discussion

The determination of the sorption mechanism on adsorbents can be achieved not only through the analysis of regular variations in adsorption isotherms and fundamental thermodynamic parameters (ΔH, ΔF, and ΔS) as a function of the amount adsorbed, but also via a comparative study of sorption parameters for adsorbates of different chemical natures. This approach enables a comprehensive characterization of the active sites of the adsorbent, their number, strength, and interaction type and allows for a deeper understanding of the adsorption mechanism.

The sorption mechanism can be characterized by examining the regular changes in the amount of adsorbed substance with respect to logarithmic coordinates of the equilibrium relative pressure and $P/P_s$ coordinates, as well as by evaluating the differential adsorption enthalpy, Gibbs free energy, and entropy, calculated using the Gibbs–Helmholtz equation. Furthermore, valuable information about the nature of the process can be obtained from thermokinetic data analysis.

In the present study, the analysis of the adsorption mechanism was limited to the adsorption isotherms plotted in logarithmic and $P/P_s$ coordinates, which made it possible to identify the main regularities governing the interaction of hydrogen sulfide with the active sites of the studied adsorbents.

At 303 K, the adsorption isotherms of hydrogen sulfide ($H_2S$) molecules were investigated on a carbon adsorbent derived from Paulownia tomentosa wood (prepared by sequential thermal pyrolysis

*Edelweiss Applied Science and Technology*
*ISSN: 2576-8484*
*Vol. 9, No. 11: 429-447, 2025*
*DOI: 10.55214/2576-8484.v9i11.10879*
*© 2025 by the authors; licensee Learning Gate*

followed by microwave activation), as well as on CaA-type zeolites synthesized by ion exchange from NaA with stoichiometries $Ca_5Na_3[(AlO_2)_{12}(SiO_2)_{12}]$ and $Ca_4Na_4[(AlO_2)_{12}(SiO_2)_{12}]$. The adsorption isotherms were approximated using the theory of volume filling of micropores (VMOT) by means of a three-parameter mathematical equation. The adsorption mechanism of hydrogen sulfide in the adsorbent pores was thoroughly analyzed from the initial region to the saturation region, up to pressures approaching the saturated vapor pressure of $H_2S$.

It should be noted that due to the high saturated vapor pressure of hydrogen sulfide ($H_2S$) molecules at 303 K ($P/P_s$=0.00004, $P_s$=17932 torr), it was not possible to obtain complete adsorption isotherms of $H_2S$ on the activated carbon adsorbent and CaA-type zeolites. Therefore, the experimental investigations were carried out in the region of low relative pressures, where the adsorption process is mainly governed by interactions between $H_2S$ molecules, micropores, and active surface sites of the adsorbents. This approach made it possible to identify the features of the initial stage of sorption and to assess the energetic heterogeneity of the active sites and their contribution to the total adsorption capacity of the studied materials.

Figure 1*a*,b presents the adsorption isotherm of hydrogen sulfide ($H_2S$) molecules on the carbon adsorbent derived from Paulownia tomentosa wood and activated by microwave irradiation, plotted in logarithmic coordinates.

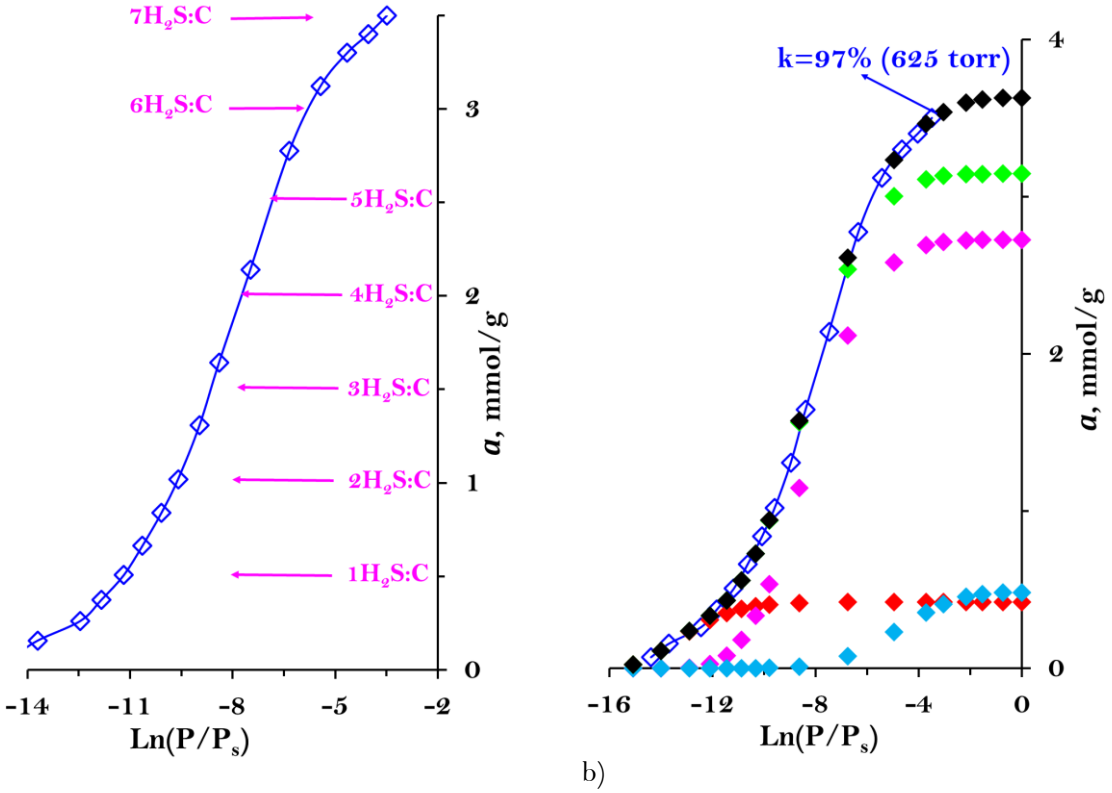


*a*) b)

**Figure 1.**
Adsorption isotherm of hydrogen sulfide ($H_2S$) molecules on an activated carbon adsorbent derived from *Paulownia tomentosa* wood at 303 K in logarithmic coordinates. ◊-experimental data; ♦,♦,♦,♦,♦-values calculated using the theory of volume filling of micropores (VMOT).

In the initial region, the isotherm exhibits a concave shape, indicating the presence of strongly interacting adsorption sites on the surface. At the initial stages of pore filling (adsorbed volume corresponding to 0.07 mmol/g), the logarithm of the relative pressure is $\ln(P/P_s)$ = -14.4 (at P = 0.01

*Edelweiss Applied Science and Technology*
*ISSN: 2576-8484*
*Vol. 9, No. 11: 429-447, 2025*
*DOI: 10.55214/2576-8484.v9i11.10879*
*© 2025 by the authors; licensee Learning Gate*

torr). The experiment was conducted up to $\ln(P/P_s) = -3.5$ (corresponding to P = 550 torr), at which point complete saturation of the adsorbent was achieved with a total amount of adsorbed hydrogen sulfide of 3.5 mmol/g.

Such isotherm behavior is typical of microporous carbon adsorbents with energetically heterogeneous surfaces and indicates sequential filling of pores of different depths and chemical nature, consistent with the mechanism of volume filling of micropores and the formation of stable adsorption complexes at the most active sites.

The adsorption isotherm of hydrogen sulfide can be conventionally divided into three characteristic regions, each reflecting a different nature of interaction between $H_2S$ molecules and the adsorbent surface. The first region (up to 0.5 mmol/g, at $\ln(P/P_s)=-11.2$, P=0.25 torr) is characterized by a concave shape of the isotherm toward the abscissa axis, indicating high-energy interactions between hydrogen sulfide molecules and the active surface sites of the adsorbent. In this range, chemisorption occurs—strong binding of molecules to active sites of various natures (acid-base, polar, or defect regions of the carbon lattice). The second region (from 0.5 to 3.0 mmol/g) exhibits an almost linear dependence, suggesting the predominance of physical adsorption within the micropores. In this range, a gradual filling of the micropore volume by $H_2S$ molecules takes place, leading to the formation of monomolecular and partially polymolecular adsorption layers. The interaction energy decreases as the most active sites become occupied, and adsorption is mainly governed by dispersion (van der Waals) forces.

The third region (up to 3.5 mmol/g) exhibits a convex bending of the isotherm toward the ordinate axis, indicating the stage of micropore saturation and the onset of $H_2S$ condensation in larger pores and interparticle spaces. At this stage, weakly bound adsorption complexes are formed, and capillary condensation may occur, which is typical at high relative pressures. Therefore, analysis of the isotherm shape reveals three sequential stages of the sorption process: chemisorption, physical adsorption in micropores, and partial condensation each reflecting the energetic heterogeneity of the surface and the structural features of the microporous adsorbent.

From the above analysis of the isotherm, it follows that the concentration of active sites on the microwave-activated carbon adsorbent with respect to hydrogen sulfide molecules is 0.5 mmol/g. This value corresponds to the concentration of the most energetic sorption centers involved in the formation of stable complexes of the type $7H_2S$/adsorbent (Fig. 1*a*), confirming the presence of strong interactions between the adsorbate and the carbon material surface.

Figures 2*a*,b present the adsorption isotherm of hydrogen sulfide ($H_2S$) molecules on a microwave-activated carbon adsorbent derived from Paulownia tomentosa wood at 303 K in relative pressure coordinates ($P/P_s$). The isotherm corresponds to Type I according to the Brunauer classification. Therefore, $H_2S$ molecules are adsorbed within the micropores of the adsorbent.

At a relative saturation pressure of $P/P_s=5.58\times10^{-7}$, the amount of adsorbed hydrogen sulfide molecules is 0.07 mmol/g. This indicates a strong adsorption binding of the initial $H_2S$ molecules to the active surface sites of the activated carbon adsorbent. As the sorption volume becomes saturated, the isotherm rises sharply along the abscissa axis. Starting from an adsorption amount of 2 mmol/g at a relative pressure of $P/P_s=5.6\times10^{-4}$, the equilibrium pressure begins to increase significantly. At this pressure, the $H_2S$ molecules form a tetrameric complex ($4H_2S$/adsorbent). From the graph (Fig. 2), it can be observed that at an adsorption amount of 3 mmol/g and a relative pressure of $P/P_s=4\times10^{-3}$, the equilibrium pressure sharply increases following the formation of a hexameric complex ($6H_2S$/adsorbent). When the adsorption reaches 3.5 mmol/g and $P/P_s=0.03$, the sorption process is completed with the formation of a heptameric complex ($7H_2S$/adsorbent).

The adsorption isotherm of hydrogen sulfide molecules on the microwave-activated carbon adsorbent derived from Paulownia tomentosa wood is described by a three-term equation based on the theory of volume filling of micropores (VMOT) [24-26, 29, 30]:

$$a=0{,}495\exp[-(A/34{,}25)^{10}] + 2{,}625\exp[-(A/22{,}41)^{5}] + 0{,}487\exp[-(A/13{,}84)^{3}] \quad (1)$$

*Edelweiss Applied Science and Technology*
*ISSN: 2576-8484*
*Vol. 9, No. 11: 429-447, 2025*
*DOI: 10.55214/2576-8484.v9i11.10879*
*© 2025 by the authors; licensee Learning Gate*

where $a$ is the amount of adsorption (mmol/g), and $\Delta G = -A = RT \ln(P_s/P)$ is the Gibbs free energy, representing the work (kJ/mol) performed in transferring the gas to the equilibrium gas phase. From Figures 1b and 2b, it is evident that the values calculated using the general equation of the volume filling of micropores theory (VMOT) correspond closely to the experimental results.

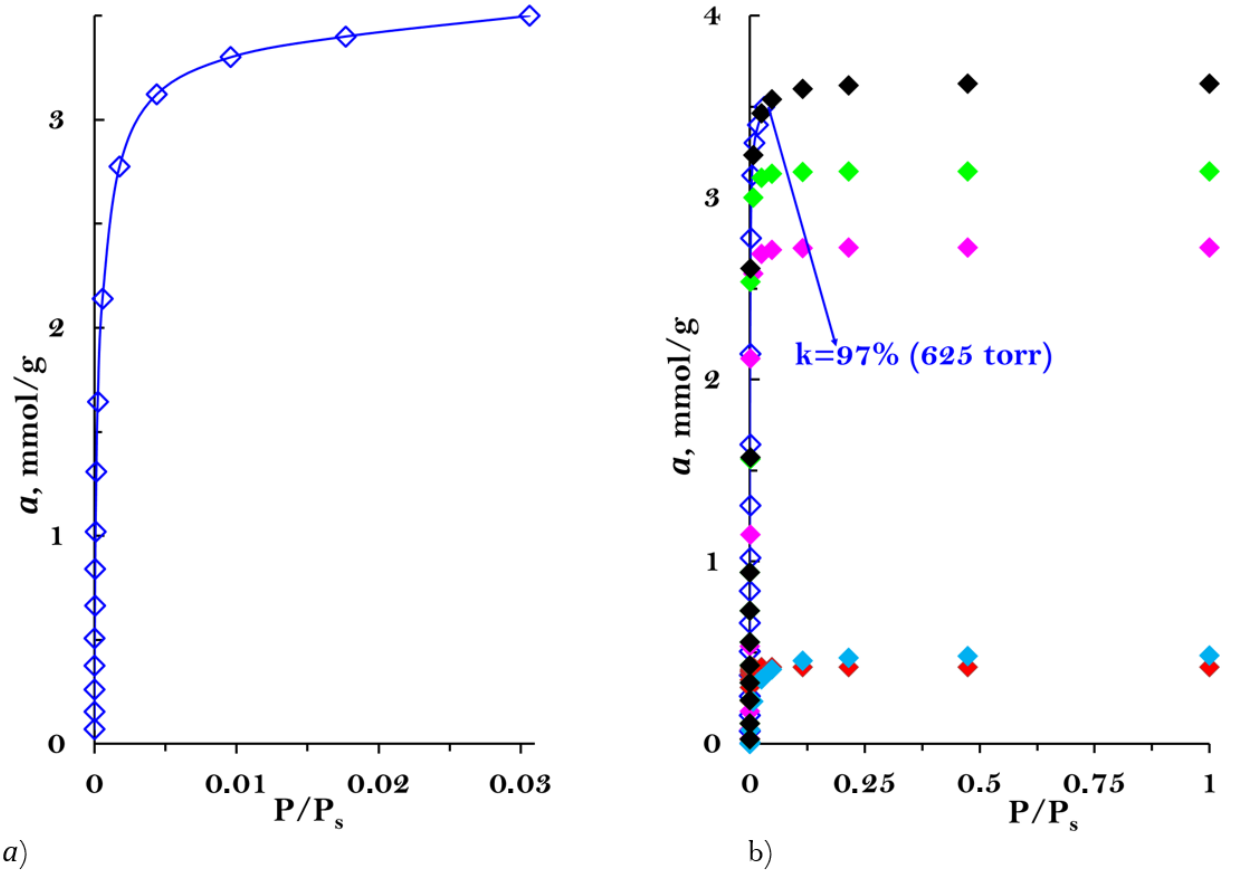


**Figure 2.**
Adsorption isotherm of hydrogen sulfide molecules on an activated carbon adsorbent derived from *Paulownia tomentosa* wood at 303 K in relative pressure coordinates. ◊-experimental data; ♦,♦,♦,♦,♦-values calculated using the theory of volume filling of micropores (VMOT).

The adsorption amounts $a_{01}$=0.495 mmol/g and $a_{02}$=0.487 mmol/g, corresponding to the first and third terms of equation (1), confirm that the number of active sorption centers of the microwave-activated carbon adsorbent, calculated from the logarithmic isotherm, is approximately 0.5 mmol/g. In Figures 1b and 2b, the symbols denote: ♦-first term of the equation, ♦-second term, ♦-third term, ♦-sum of the first and second terms, and ♦-sum of all three terms.

The value $a_{02}$=2.625 mmol/g corresponds to the linear section of the isotherm in the adsorption range from 0.5 to 3.0 mmol/g. Therefore, the adsorption coefficients ($a_{01}$, $a_{02}$, $a_{03}$), calculated using equation (1) based on the VMOT, reflect the sequential formation of adsorption complexes from a monomer ($1H_2S$/adsorbent) to a dimer ($2H_2S$/adsorbent) and further to a hexamer ($6H_2S$/adsorbent). The sharp rise in equilibrium pressure corresponds to the formation of a heptamer complex ($7H_2S$/adsorbent), marking the completion of the $H_2S$ adsorption process on this adsorbent.

Based on equation (1), the $H_2S$ isotherm was theoretically calculated up to the saturation pressure (Figs. 1b, 2b). At saturation, the theoretically calculated adsorption capacity according to the VMOT

*Edelweiss Applied Science and Technology*
*ISSN: 2576-8484*
*Vol. 9, No. 11: 429-447, 2025*
*DOI: 10.55214/2576-8484.v9i11.10879*
*© 2025 by the authors; licensee Learning Gate*

equation was 3.63 mmol/g, while the experimentally determined value at $P/P_s$=0.03 (P=550 torr) was 3.5 mmol/g. Thus, the saturation coefficient at experimental conditions is k=97%, indicating that the activated carbon adsorbent derived from Paulownia tomentosa can be effectively used for hydrogen sulfide removal under normal atmospheric pressure.

In various industrial sectors, the use of natural adsorbents alone is often insufficient. Therefore, synthetic zeolites are widely applied. In this study, along with activated carbon adsorbents, adsorption isotherms of hydrogen sulfide on CaA-type zeolites with different cation compositions—$Ca_4Na_4[(AlO_2)_{12}(SiO_2)_{12}]$ and $Ca_5Na_3[(AlO_2)_{12}(SiO_2)_{12}]$ are also presented.

The adsorption isotherm of hydrogen sulfide on the $Ca_4Na_4$ ($CaA_{II}$) zeolite in logarithmic coordinates is shown in Figures 3a,b. At low degrees of pore filling (0.091 mmol/g), the logarithm of the relative equilibrium pressure is $\ln(P/P_s)$ = -13.71 (P = 0.02 torr). Here, $P_s$ = 17,936 torr corresponds to the saturated vapor pressure of hydrogen sulfide at the experimental temperature (303 K). Due to the high vapor pressure of $H_2S$, the experiments were conducted up to P = 627 torr. At this pressure, the isotherm reaches $\ln(P/P_s)$ = -3.2, corresponding to an adsorption capacity of 5.44 mmol/g.

The chemical composition of the $Ca_4Na_4$ zeolite indicates that the total number of sodium and calcium cations, i.e., the main active centersmequals 1.1 mmol/g. Therefore, the adsorption isotherm of hydrogen sulfide on this zeolite is expected to exhibit a stepwise pattern, corresponding to the number of cations (1.1 mmol/g) present in the structure of the adsorbent.

Figure 2*a* shows the adsorption isotherm of hydrogen sulfide ($H_2S$) on the $Ca_4Na_4$-$A_I$ zeolite, plotted in logarithmic coordinates as the dependence of the amount of adsorbed gas on the logarithm of the relative pressure, $\ln(P/P_s)$. The isotherm exhibits a smoothly increasing, S-shaped profile and consists of several sequential regions corresponding to the formation of coordination complexes of the composition $mH_2S$: $CaA_I$ (m=1–5).

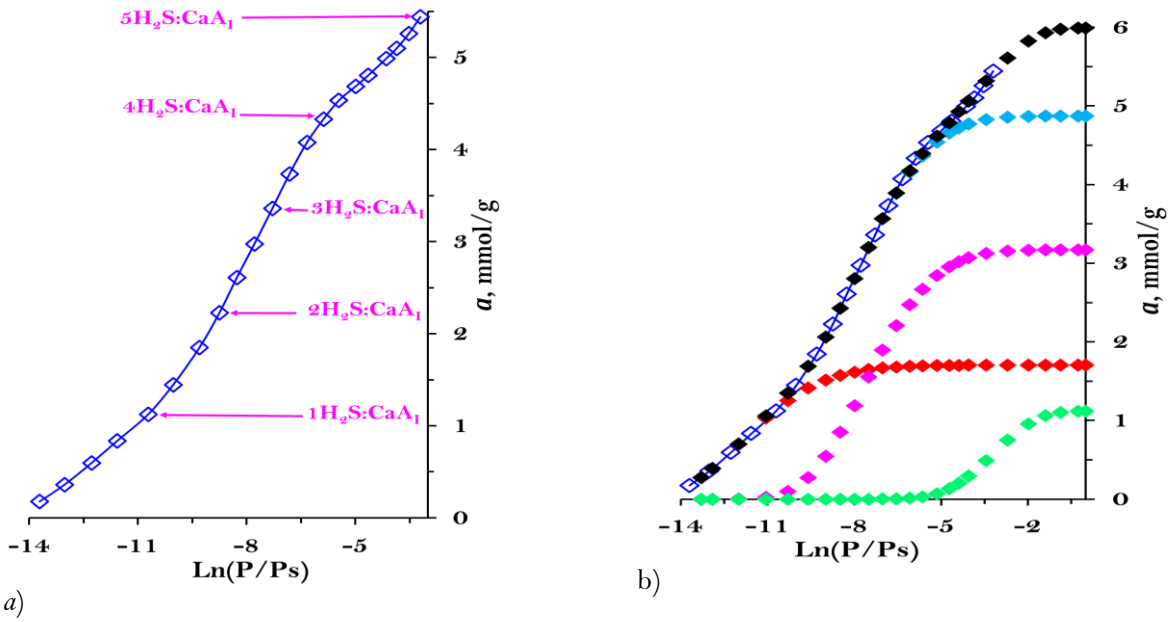


*a*) b)

**Figure 3.**

Adsorption isotherm of hydrogen sulfide on the $Ca_4Na_4$ zeolite at 303 K in logarithmic coordinates. ◊- experimental data; ♦,♦,♦,♦,♦- values calculated using the theory of volume filling of micropores (VMOT).

At low pressures ($\ln(P/P_s) < -12$), a linear relationship is observed, characteristic of the Henry region. In this range, adsorption is governed by strong interactions between $H_2S$ molecules and $Na^+$ and $Ca^{2+}$ cations localized at the α-sites of the zeolite framework. At this stage, a primary complex $1H_2S$: $CaA_I$ is formed, the amount of which corresponds to the number of active adsorption centers (1.1

*Edelweiss Applied Science and Technology*
*ISSN: 2576-8484*
*Vol. 9, No. 11: 429-447, 2025*
*DOI: 10.55214/2576-8484.v9i11.10879*
*© 2025 by the authors; licensee Learning Gate*

mmol/g). With further increases in relative pressure, additional $H_2S$ molecules successively attach to each active center, leading to the formation of a series of complexes: $2H_2S$: $CaA_I$, $3H_2S$: $CaA_I$, $4H_2S$: $CaA_I$, and $5H_2S$: $CaA_I$. The maximum adsorption reaches approximately 5.5 mmol/g, corresponding to the binding of up to five hydrogen sulfide molecules by the sodium and calcium cations.

This behavior indicates a cluster-type adsorption mechanism**:** the first $H_2S$ molecule forms a strong coordination bond with the $Ca^{2+}$ ion, while subsequent molecules are retained through hydrogen bonding and dipole–dipole interactions within a localized cluster. For each successive molecule, the binding energy decreases, and thus their attachment requires higher pressure. This phenomenon is reflected in the multistep shape of the isotherm**.**

Figures 4*a*, b show the adsorption isotherm of hydrogen sulfide ($H_2S$) molecules on the $Ca_4Na_4$ zeolite at 303 K in relative pressure coordinates ($P/P_s$). The isotherm corresponds to Type I according to the Brunauer classification. Therefore, $H_2S$ molecules are adsorbed in the micropores of the zeolite.

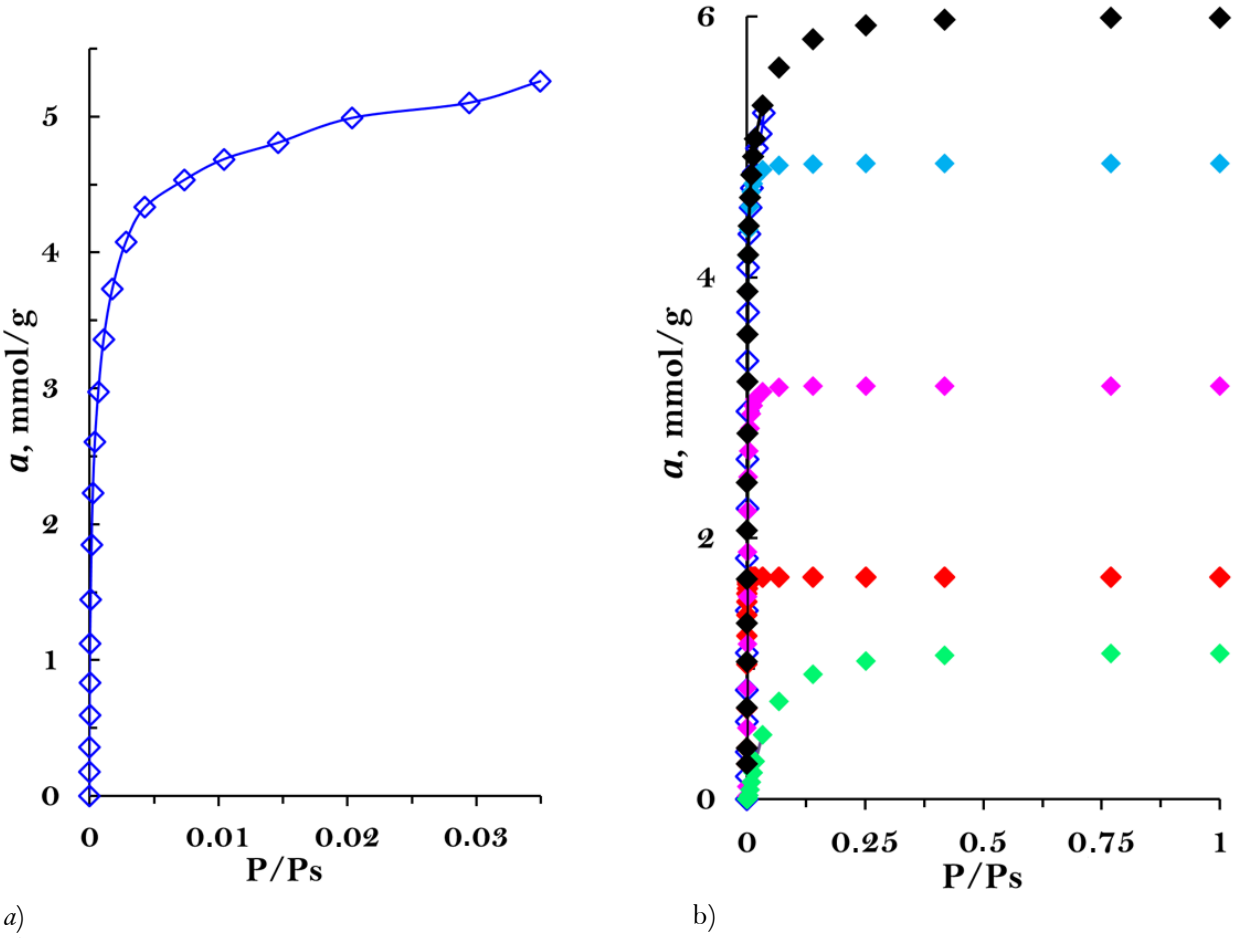


*a*) b)

**Figure 4.**

Adsorption isotherm of hydrogen sulfide molecules on the $Ca_4Na_4$ zeolite at 303 K in relative pressure coordinates. ◊-experimental data; ♦,♦,♦,♦,♦-values calculated using the theory of volume filling of micropores (VMOT).

Figure 4*a* shows the adsorption isotherm of hydrogen sulfide ($H_2S$) on the $Ca_4Na_4$ zeolite at 303 K. The curve exhibits a distinctly convex upward shape, corresponding to a Type I isotherm according to the IUPAC classification. This type of isotherm is typical for microporous adsorbents (such as zeolites

*Edelweiss Applied Science and Technology*
*ISSN: 2576-8484*
*Vol. 9, No. 11: 429-447, 2025*
*DOI: 10.55214/2576-8484.v9i11.10879*
*© 2025 by the authors; licensee Learning Gate*

and carbons with micropores smaller than 2 nm), in which adsorption at low relative pressures ($P/P_s<0.03$) is governed by rapid filling of the micropore volume.

In the initial region ($P/P_s<0.005$), a sharp increase in adsorption is observed, indicating the presence of high-energy sorption centers associated with $Ca^{2+}$ and $Na^+$ cations located within the zeolite framework. At this stage, $H_2S$ molecules are strongly bound to these cationic sites. As the relative pressure increases, the adsorption growth slows down, and at $P/P_s\approx0.02$-$0.03$, a plateau is reached corresponding to the complete filling of the micropores. The maximum adsorption capacity is approximately 5.2-5.4 mmol/g, which is equivalent to about 180 mg of $H_2S$ per gram of sorbent.

The primary adsorption mechanism of $H_2S$ on these zeolites is physisorption, where the interaction between $H_2S$ molecules and the surface mainly occurs through electrostatic and polarization effects. $Ca^{2+}$ cations have a high polarizing power, inducing a dipole in $H_2S$ molecules and thereby strengthening van der Waals interactions. The contribution of $Na^+$ cations to polarization is significantly weaker; consequently, adsorption predominantly occurs at sites containing $Ca^{2+}$.

At low pressures, $H_2S$ molecules are strongly retained near these cations. As these sites become occupied, further pressure increases lead to filling of less energetically favorable micropores, which manifests as the gradual leveling of the isotherm toward a plateau. The shape of the isotherm (rapid rise → slowdown → plateau) reflects the energetic heterogeneity of the adsorption surface. This can be described using the Toth or Sips models, which account for variations in binding energy at different types of adsorption sites. In this case, at least two types of sites can be distinguished:
- Strong sites - $Ca^{2+}$ cations and adjacent framework regions with high binding energy;
- Weak sites - porous regions between aluminosilicate tetrahedra with lower binding energy. Thus, at low pressures, adsorption occurs primarily on strong sites, while at higher pressures, less active regions are gradually filled.

At 303 K, adsorption is predominantly physical in nature; however, the presence of divalent $Ca^{2+}$ cations may lead to partial ion exchange and somewhat stronger fixation of $H_2S$. Increasing the temperature would reduce adsorption capacity, confirming the physical nature of the interaction, whereas decreasing the temperature could enhance adsorption by 10–20%. The $Ca^{2+}/Na^+$ ratio plays a critical role: increasing the $Ca^{2+}$ content strengthens the electrostatic field and enhances interaction with $H_2S$, whereas an excess of $Na^+$ reduces capacity and shifts the isotherm toward lower pressures.

For comparison, typical $H_2S$ adsorption capacities at 303 K are 0.5-2.0 mmol/g for activated carbons and 3-4 mmol/g for NaY-type zeolites. Thus, the $Ca_4Na_4$ zeolite exhibits a significantly higher sorption capacity (up to 5.4 mmol/g), demonstrating its high efficiency for gas purification from $H_2S$ even at low partial pressures.

The sharp adsorption rise at low pressures ($P/P_s<0.01$) indicates that $Ca_4Na_4$ zeolite is particularly effective for deep purification of gases such as natural gas, biogas, and synthesis gas from trace amounts of hydrogen sulfide. Due to its high capacity and reversible physisorption behavior, the adsorbent can be easily regenerated by simple heating or purging with an inert gas.

Therefore, $Ca_4Na_4$ zeolite can be considered a promising material for low-temperature adsorption columns, offering high selectivity and stability under multiple adsorption-desorption cycles.

The adsorption isotherm of hydrogen sulfide ($H_2S$) molecules on the $Ca_4Na_4$ zeolite is described by a three-term equation of the Theory of Volume Filling of Micropores (VMOT) [24-26, 29, 30]:

$$a=1{,}7\exp[-(A/30{,}72)^7] + 3{,}17\exp[-(A/20{,}21)^5] + 1{,}12\exp[-(A/9{,}24)^3] \quad (2)$$

From Figures 3b and 4b, it is evident that the values calculated based on the general equation of the Volume Filling of Micropores Theory (VMOT) are in complete agreement with the experimentally obtained data.

The first term of Equation (2), corresponding to $a_{01}=1.7$ mmol/g, accurately describes the experimental isotherm up to an adsorption value of 1.1 mmol/g. Furthermore, the third term of Equation (2) is equal to $a_{03}=1.12$ mmol/g. These values correspond to the total number of cations

*Edelweiss Applied Science and Technology*
*ISSN: 2576-8484*
*Vol. 9, No. 11: 429-447, 2025*
*DOI: 10.55214/2576-8484.v9i11.10879*
*© 2025 by the authors; licensee Learning Gate*

present in the chemical composition of the zeolite. Hence, the VMOT theory confirms that on the $Ca_4Na_4$ zeolite, $H_2S$ molecules form sequential ion–molecular adsorbate/cation complexes ranging from monomer to pentamer, such as ($1H_2S$: $CaA_I$), ($2H_2S$: $CaA_I$), ($3H_2S$: $CaA_I$), ($4H_2S$: $CaA_I$), and ($5H_2S$: $CaA_I$).

Based on Equation (2), the adsorption isotherm was theoretically calculated up to the saturation pressure of $H_2S$ (Figures 3b and 4b). At the saturation pressure of 17,936 torr, the theoretically calculated adsorption value according to the VMOT equation is 6 mmol/g, whereas the experimentally measured adsorption value at $P/P_s$=0.04 (P=627 torr) is 5.4 mmol/g. Therefore, the saturation coefficient under experimental pressure is k=90%, which demonstrates that the $Ca_4Na_4$ zeolite can be effectively used for hydrogen sulfide removal in various industrial applications under normal atmospheric pressure.

The sorption properties of zeolites of the LTA type, including CaA zeolites, vary depending on the ratio of calcium and sodium cations in their structure. For this reason, the present study includes both experimentally obtained and theoretically calculated isotherms of hydrogen sulfide ($H_2S$) adsorption on the zeolite $Ca_5Na_3[(AlO_2)_{12}(SiO_2)_{12}]$ ($CaA_{II}$), determined using the Theory of Volume Filling of Micropores (VMOT) equation.

Due to the unequal number of calcium and sodium cations in the composition of this zeolite, the theoretical description of the sorption mechanism presents certain difficulties. The logarithmic adsorption isotherm of hydrogen sulfide on the $Ca_5Na_3$ ($CaA_{II}$) zeolite is shown in Figures 5a and 5b. At low degrees of pore filling, corresponding to an adsorption amount of 0.14 mmol/g, the logarithm of the equilibrium relative pressure is $Ln(P/P_s)$ = -14.72 (P = 0.0073 torr). Because of the higher partial pressure of hydrogen sulfide, the experiments were conducted up to P = 677 torr.

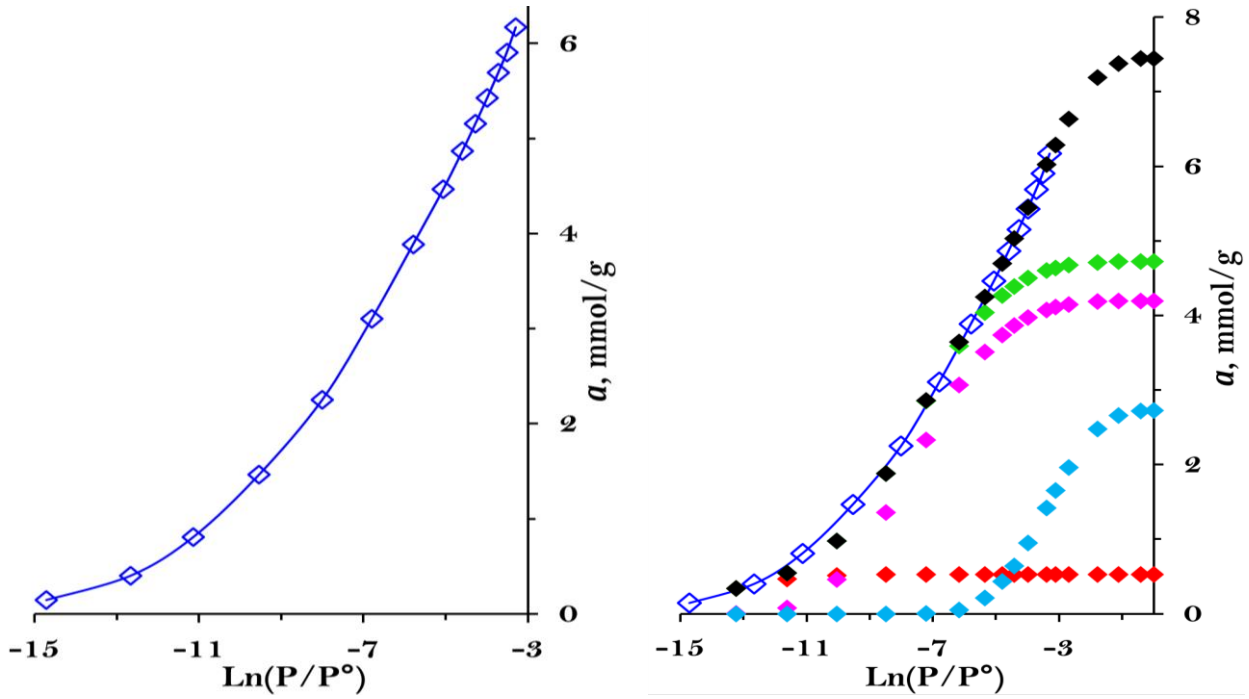


*a*) b)

**Figure 5.**

Adsorption isotherm of hydrogen sulfide on the $Ca_5Na_3$ zeolite at 303 K in logarithmic coordinates. ◊- experimental data; ♦,♦,♦,♦,♦- values calculated using the theory of volume filling of micropores (VMOT).

Under these conditions, the adsorption isotherm reached $Ln(P/P_s)$ = -3.3, corresponding to an adsorption amount of 6.17 mmol/g. This adsorption capacity is 0.8 mmol/g higher than that of $Ca_4Na_4$

*Edelweiss Applied Science and Technology*
*ISSN: 2576-8484*
*Vol. 9, No. 11: 429-447, 2025*
*DOI: 10.55214/2576-8484.v9i11.10879*
*© 2025 by the authors; licensee Learning Gate*

($CaA_I$) zeolite, indicating that the sorption volume of $Ca_4Na_4$ ($CaA_{II}$) is greater than that of $Ca_4Na_4$ ($CaA_I$).

Figure 5 shows the adsorption isotherm of hydrogen sulfide ($H_2S$) molecules on the zeolite $Ca_5Na_3[(AlO_2)_{12}(SiO_2)_{12}]$ at 303 K, plotted in logarithmic coordinates $\ln(P/P_s)$. The curve exhibits a smooth upward trend typical of microporous adsorbents. This type of isotherm corresponds to Type I according to the IUPAC classification and reflects a monolayer filling of micropores. The logarithmic form of the dependence clearly reveals the exponential growth of the adsorbed amount in the low-pressure region, indicating a high adsorption energy of $H_2S$ on active sites and the presence of a narrow-pore structure in the zeolite.

The $Ca_5Na_3$ ($CaA_{II}$) zeolite contains $Ca^{2+}$ and $Na^+$ cations located in the cavities of the aluminosilicate framework. These cations create local electrostatic fields capable of polarizing $H_2S$ molecules, which possess a dipole moment of 0.97 D. As a result, ion–dipole interactions are formed between $H_2S$ molecules and the cationic centers of the zeolite.

The divalent calcium cation makes the predominant contribution to the retention of $H_2S$ molecules because of its higher polarizing ability compared with $Na^+$. At the initial stage (low pressures), $H_2S$ molecules are adsorbed on the most energetically favorable sites associated with $Ca^{2+}$; as these sites become occupied, the process continues on less active $Na^+$ centers. Thus, the adsorption process is of a physisorption nature, but it exhibits a pronounced specificity due to the electrostatic interactions with cationic sites.

The shape of the isotherm in logarithmic coordinates indicates the existence of energetically heterogeneous regions on the surface. In the initial region ($\ln P/P_s<-13$), adsorption changes only slightly, corresponding to the filling of very strong sites. In the range $-13<\ln P/P_s<-8$, the adsorption rate increases sharply, reflecting the active filling of micropores. With further pressure increase ($\ln P/P_s>-8$), the adsorption rate decreases as equilibrium is approached and the microporous volume becomes fully occupied.

A comparison with the $Ca_4Na_4$ zeolite shows that increasing the calcium content to $Ca_5Na_3$ raises the adsorption capacity from 5.4 to 6.2 mmol/g. This increase is attributed to the higher number of high-energy $Ca^{2+}$ sites with greater polarizing ability. Therefore, modifying the cationic composition significantly influences the sorption properties of the zeolite, enhancing both the capacity and the equilibrium constant (adsorption energy).

The adsorption energy, obtained from the slope of the linear section of the isotherm, confirms the physical nature and reversibility of the process. This indicates that $H_2S$ desorption can occur upon moderate heating (up to 400 K), making the zeolite suitable for multiple regeneration cycles.

Due to its high capacity at low pressures ($P/P_s<10^{-4}$), the $Ca_5Na_3$ ($CaA_{II}$) zeolite is a promising material for deep purification of gases from hydrogen sulfide. It surpasses activated carbons and NaY-type aluminosilicates in efficiency and selectivity at low partial pressures of $H_2S$.

The analysis of the $H_2S$ adsorption isotherm on $Ca_5Na_3$ ($CaA_{II}$) at 303 K demonstrates that the process follows a micropore-filling model and is characterized by monolayer physisorption with elements of specific interaction at cationic sites. Increasing the calcium content strengthens the electrostatic interaction and enhances the adsorption capacity of the material.

Thus, the $Ca_5Na_3$ zeolite can be classified as a highly efficient adsorbent for the selective removal of hydrogen sulfide from natural gas, biogas, and industrial mixtures at low pressures. Its high capacity, thermal stability, and regeneration capability ensure its practical applicability in industrial gas purification processes.

The adsorption isotherm of $H_2S$ molecules on the $Ca_5Na_3$ zeolite at a temperature of 303 K in the coordinates of relative pressure $P/P_s$ is shown in Figures 6a and 6b**.** The isotherm corresponds to Type I according to the Brunauer classification**,** indicating that $H_2S$ molecules are adsorbed within the micropores of the zeolite.

*Edelweiss Applied Science and Technology*
*ISSN: 2576-8484*
*Vol. 9, No. 11: 429-447, 2025*
*DOI: 10.55214/2576-8484.v9i11.10879*
*© 2025 by the authors; licensee Learning Gate*

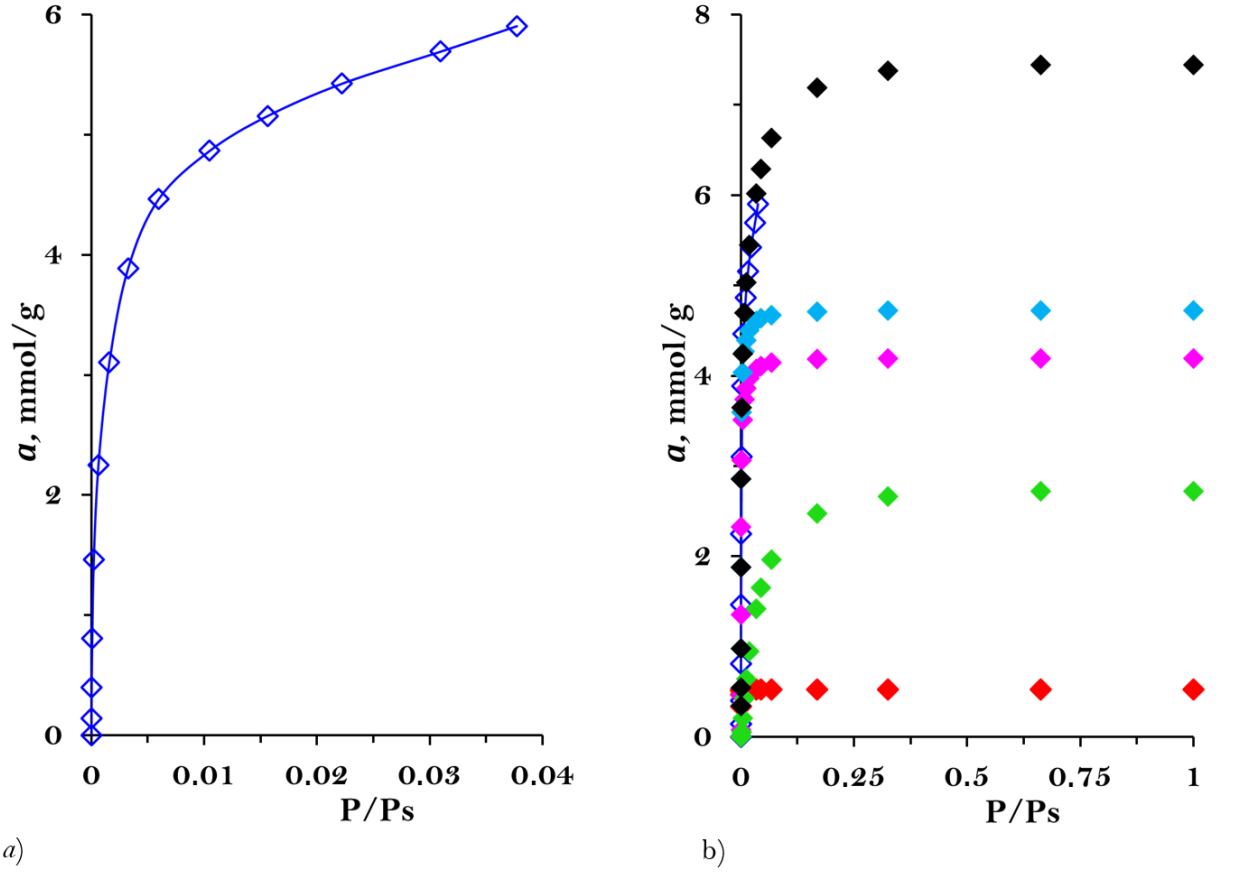


**Figure 6.**

Adsorption isotherm of hydrogen sulfide molecules on the $Ca_5Na_3$zeolite at 303 K in relative pressure coordinates. ◊-experimental data; ♦,♦,♦,♦,♦-values calculated using the theory of volume filling of micropores (VMOT).

Figure 6 presents the adsorption isotherm of hydrogen sulfide ($H_2S$) on the zeolite $Ca_5Na_3[(AlO_2)_{12}(SiO_2)_{12}]$ (hereafter referred to as $CaA_{II}$) at 303 K, plotted in $P/P_s$ coordinates. The curve exhibits a pronounced convex shape characteristic of Type I isotherms according to the IUPAC classification. This type of isotherm is typical of microporous adsorbents, in which adsorption occurs due to the rapid filling of micropores at low relative pressures ($P/P_s < 0.03$). As the relative pressure increases from 0 to 0.03, adsorption rises sharply to approximately 5.5-5.6 mmol/g, after which the curve levels off into a plateau. This indicates the attainment of equilibrium, where most of the micropores are filled with $H_2S$ molecules. Such behavior is characteristic of sorbents with high microporosity and limited mesoporous volume.

The $Ca_5Na_3$ zeolite possesses an LTA-type aluminosilicate framework containing divalent $Ca^{2+}$ and monovalent $Na^+$ cations located within the lattice cavities. These cations generate local electrostatic fields that interact with the polar $H_2S$ molecules. Due to the high polarizing power of $Ca^{2+}$, adsorption predominantly occurs via the ion–dipole interaction mechanism, in which the $H_2S$ molecule is oriented toward the cationic center. Therefore, the process is of a physisorptive nature, but it is accompanied by pronounced selectivity and relatively high binding energy. At low relative pressures ($P/P_s<0.01$), the pore filling occurs mainly at high-energy sites associated with $Ca^{2+}$ cations, while at higher pressures, less energetic sites such as pores containing $Na^+$ and framework regions become involved.

The sharp increase in adsorption at low pressures indicates a high interaction energy between $H_2S$ and the active sites of the zeolite. As the pressure increases further, the adsorption rate gradually

*Edelweiss Applied Science and Technology*
*ISSN: 2576-8484*
*Vol. 9, No. 11: 429-447, 2025*
*DOI: 10.55214/2576-8484.v9i11.10879*
*© 2025 by the authors; licensee Learning Gate*

decreases due to the saturation of the microporous volume. Such behavior corresponds to a heterogeneous system with a distribution of adsorption sites by binding energy. The dependence can be quantitatively described by the Langmuir equation. The obtained data yield a maximum adsorption capacity of approximately $a_m \approx 5.6$ mmol/g and an adsorption energy E≈40 kJ/mol, which is characteristic of strong physical adsorption without chemical bond formation.

In comparison with the $Ca_4Na_4$ zeolite, increasing the calcium content to $Ca_5Na_3$ results in an increase in adsorption capacity (from 5.4 to 6.2 mmol/g). This effect is attributed to: a greater number of high-energy $Ca^{2+}$ sites in the micropores; strengthening of the local electrostatic field; and enhanced polarization of $H_2S$ molecules near the active regions.

Thus, increasing the proportion of divalent cations strengthens the interaction between the adsorbate and the internal surface of the zeolite, leading to more efficient utilization of the microporous volume. In addition, the $CaA_{II}$ zeolite exhibits a more rigid framework, which contributes to the stability of its sorption properties during adsorption–desorption cycles.

The shape of the isotherm confirms monolayer micropore filling without any indication of capillary condensation. This suggests that $H_2S$ adsorption occurs in microporous channels less than 1 nm in diameter, where the interaction between the molecules and the surface dominates over intermolecular forces. The adsorption energy (~40 kJ/mol) confirms the reversible nature of the process, enabling regeneration of the adsorbent either by moderate heating (up to approximately 400 K) or by vacuum desorption. Owing to its high capacity at low pressures, the $Ca_5Na_3$ zeolite can be recommended for deep purification of natural gas and biogas from $H_2S$, particularly under low concentration conditions and temperatures around 300 K.

Analysis of the adsorption isotherm and calculated parameters shows that the adsorption energy of $H_2S$ lies within the range of 35-45 kJ/mol, confirming the reversible character of the process. Therefore, $H_2S$ desorption can be achieved by mild heating (≈400 K) or by vacuum regeneration. The high adsorption capacity of the $CaA_{II}$ zeolite at low pressures makes it a promising material for deep gas purification, showing high selectivity for $H_2S$ over $CO_2$ and $H_2O$, which is especially important for multiphase gas mixtures.

The obtained isotherms are consistent with the findings of other researchers. Starke et al. [31] and Starke et al. [32] demonstrated that increasing the $Ca^{2+}$ content in LTA- and FAU-type zeolites enhances $H_2S$ sorption capacity by more than 20%. Yu et al. [33] noted that for zeolites with micropores smaller than 1 nm, a typical Type I isotherm with a steep saturation at $P/P_s<0.05$ is observed. Similar dependencies were reported in Georgiadis et al. [34] and Abdurakhmonov and Dekhkanova [35], confirming the validity of the experimental results obtained in this work.

The analysis of the $H_2S$ adsorption isotherm on the $Ca_5Na_3[(AlO_2)_{12}(SiO_2)_{12}]$ ($CaA_{II}$) zeolite at 303 K demonstrates that the process follows the micropore monolayer filling mechanism, which is primarily driven by electrostatic interactions between $H_2S$ molecules and $Ca^{2+}$ cations. The observed maximum capacity of 6.2 mmol/g and high selectivity indicate that this material is an efficient adsorbent for $H_2S$ removal from gas mixtures. Increasing the $Ca^{2+}$ content within the zeolite framework enhances both the interaction energy and the sorption capacity, offering opportunities for targeted modifications of zeolite structures to optimize gas purification applications.

Figure 7 shows the adsorption isotherms of hydrogen sulfide ($H_2S$) molecules on zeolites $Ca_4Na_4[(AlO_2)_{12}(SiO_2)_{12}]$, $Ca_5Na_3[(AlO_2)_{12}(SiO_2)_{12}]$, and a plant-derived Tomentose adsorbent at 303 K. All dependencies exhibit an exponential form corresponding to Type I(a) according to the IUPAC classification, which is typical of microporous adsorbents. Differences in the position and slope of the curves reflect the influence of cation composition and surface structure on the sorption behavior.

The Ca-Na zeolites demonstrate significantly higher capacities compared to the organic-mineral Tomentose adsorbent. The $Ca_5Na_3$ zeolite achieves a maximum adsorption of 6.1 mmol/g, while $Ca_4Na_4$ reaches approximately 5.4 mmol/g. In contrast, the Tomentose adsorbent shows a markedly lower capacity of about 3.5 mmol/g. This difference arises from both the microporous nature of the zeolites

*Edelweiss Applied Science and Technology*
*ISSN: 2576-8484*
*Vol. 9, No. 11: 429-447, 2025*
*DOI: 10.55214/2576-8484.v9i11.10879*
*© 2025 by the authors; licensee Learning Gate*

and the presence of $Ca^{2+}$ and $Na^{+}$ cations, which create local electrostatic fields that promote polarization of $H_2S$ molecules.

An increase in the proportion of divalent calcium cations from $Ca_4Na_4$ to $Ca_5Na_3$ enhances the number of high-energy adsorption sites and strengthens ion–dipole interactions. This is manifested as a steeper initial section of the isotherm and an upward shift of the curve along the *a*-axis. Therefore, the $Ca_5Na_3$ zeolite exhibits the highest affinity for $H_2S$, ensuring more complete micropore filling at low pressures ($\ln P/P_s$ - 10).

In contrast, the Tomentose adsorbent shows weaker interaction energy due to its predominantly meso- and macroporous structure and the absence of cationic sites capable of efficiently polarizing $H_2S$ molecules. Its isotherm shows a smoother rise and earlier saturation, typical of physically adsorbing surfaces without pronounced ion-exchange activity.

In summary, the obtained results confirm that Ca-Na zeolites are highly effective $H_2S$ adsorbents and that increasing the calcium content enhances sorption properties by increasing the number of active cationic sites. While the Tomentose adsorbent may be used as an inexpensive but low-capacity material for preliminary gas purification, the $Ca_5Na_3$ zeolite shows clear potential for deep, selective $H_2S$ adsorption at low partial pressures.

Figure 8 shows the adsorption isotherms of hydrogen sulfide ($H_2S$) at 303 K on the zeolites $Ca_4Na_4[(AlO_2)_{12}(SiO_2)_{12}]$, $Ca_5Na_3[(AlO_2)_{12}(SiO_2)_{12}]$, and on the Tomentose adsorbent derived from plant material. All three isotherms correspond to Type I(a) according to the **I**UPAC classification**,** indicating predominant microporous adsorption and a monolayer pore-filling process**.**

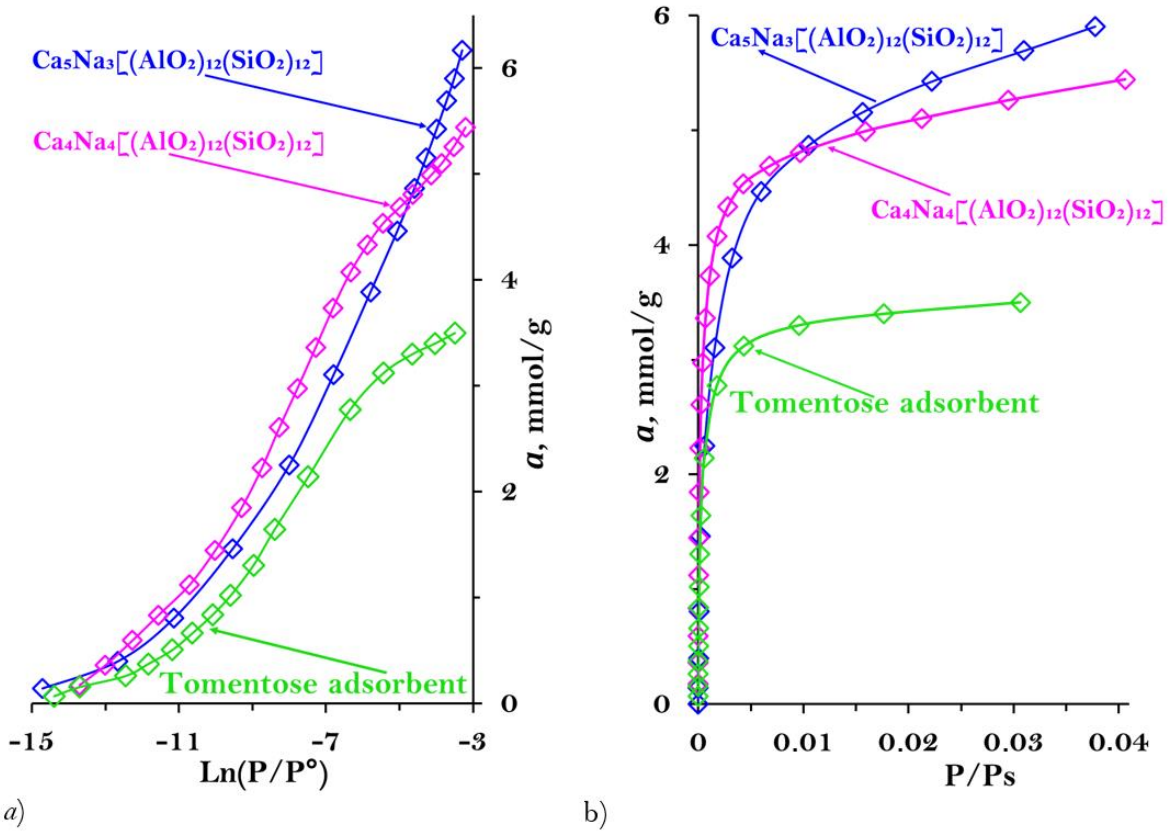


**Figure 7.**
Adsorption isotherms of hydrogen sulfide molecules on carbon adsorbent and CaA-type zeolites.

*Edelweiss Applied Science and Technology*
*ISSN: 2576-8484*
*Vol. 9, No. 11: 429-447, 2025*
*DOI: 10.55214/2576-8484.v9i11.10879*
*© 2025 by the authors; licensee Learning Gate*

Ca-Na-type zeolites are characterized by a sharp increase in adsorption at low relative pressures (P/Ps<0.01), which is associated with the presence of high-energy cationic centers ($Ca^{2+}$ and $Na^{+}$) within the aluminosilicate framework. For the $Ca_4Na_4$ zeolite, the maximum adsorption reaches approximately 5.2 mmol/g, while for $Ca_5Na_3$, it increases to 5.7-5.8 mmol/g, indicating a higher adsorption capacity with an increasing proportion of divalent calcium cations. The higher content of $Ca^{2+}$ strengthens the electrostatic field inside the micropores and enhances the polarization of $H_2S$ molecules, resulting in stronger and more selective retention.

In comparison, the Tomentose adsorbent exhibits a significantly lower sorption capacity—not exceeding 3.2-3.5 mmol/g. The corresponding isotherm shows a less pronounced slope and earlier saturation, indicating a meso- or macroporous structure with a low density of active sites. Unlike zeolites, the structure of the plant-based adsorbent lacks ionic sites capable of effectively polarizing $H_2S$ molecules; therefore, the process is limited to weak physical adsorption.

Thus, comparative analysis shows that Ca-Na-type zeolites far outperform the natural organo-mineral adsorbent in both adsorption capacity and interaction energy. An increase in calcium content along the $Ca_4Na_4 \rightarrow Ca_5Na_3$ series enhances the sorption activity and binding energy, confirming the crucial role of cationic composition in determining sorption properties. From a practical standpoint, the $Ca_5Na_3$ zeolite is the most effective adsorbent for selective $H_2S$ removal at low pressures and room temperature, whereas the Tomentose adsorbent can be used only for preliminary gas purification stages.

Ca-Na-type zeolites exhibit a pronounced increase in adsorption at low relative pressures ($P/P_s<0.01$), which is associated with the presence of high-energy cationic centers ($Ca^{2+}$ and $Na^{+}$) within the aluminosilicate framework. For the $Ca_4Na_4$ zeolite, the maximum adsorption reaches approximately 5.2 mmol/g, while for $Ca_5Na_3$, it increases to 5.7–5.8 mmol/g, indicating a higher adsorption capacity with the increasing proportion of divalent calcium cations. The higher $Ca^{2+}$ content strengthens the electrostatic field inside the micropores and enhances the polarization of $H_2S$ molecules, leading to stronger and more selective retention.

In comparison, the Tomentose adsorbent exhibits a significantly lower sorption capacity - not exceeding 3.0-3.2 mmol/g. Its isotherm shows a gentler slope and an earlier saturation, indicating a meso- or macroporous structure with a low density of active sites. Unlike zeolites, the structure of the plant-based adsorbent lacks ionic sites capable of effectively polarizing hydrogen sulfide molecules; therefore, the adsorption process is limited to weak physical interactions.

Thus, comparative analysis shows that Ca-Na-type zeolites significantly outperform the natural organo-mineral adsorbent in both adsorption capacity and interaction energy. An increase in calcium content along the $Ca_4Na_4 \rightarrow Ca_5Na_3$ series enhances the sorption activity and binding energy, confirming the critical role of the cationic composition in shaping the sorption properties. From a practical perspective, the $Ca_5Na_3$ zeolite is the most efficient adsorbent for the selective removal of $H_2S$ under low-pressure and ambient temperature conditions, whereas the Tomentose adsorbent can be used only for preliminary gas purification stages.

**Table 1.**
Comparative parameters of $H_2S$ adsorption at 303 K.

| **Adsorbent** | **Maximum capacity $a_m$, mmol·g$^{-1}$** | **Isotherm type (according to IUPAC)** | **Nature of interaction** | **Pore structure characteristics** |
|---|---|---|---|---|
| $Ca_5Na_3[(AlO_2)_{12}(SiO_2)_{12}]$ | 6 – 6.2 | I(a) | Ion–dipole physisorption ($Ca^{2+}$ > $Na^{+}$) | Microporous, high-energy |
| $Ca_4Na_4[(AlO_2)_{12}(SiO_2)_{12}]$ | 5.2 – 5.4 | I(a) | Physisorption involving $Ca^{2+}$ and $Na^{+}$ | Microporous, moderately heterogeneous |
| Tomentose adsorbent | 3.3 – 3.5 | I(b) | Weak physisorption (van der Waals forces) | Meso- and macroporous, low-energy |

*Edelweiss Applied Science and Technology*
*ISSN: 2576-8484*
*Vol. 9, No. 11: 429-447, 2025*
*DOI: 10.55214/2576-8484.v9i11.10879*
*© 2025 by the authors; licensee Learning Gate*

Table 1 presents the comparative parameters of hydrogen sulfide ($H_2S$) adsorption at a temperature of 303 K on an activated carbon adsorbent derived from Tomentose wood and on LTA-type zeolites.

Table 1 presents the comparative parameters of hydrogen sulfide ($H_2S$) adsorption at 303 K on CaA-type zeolites with different $Ca^{2+}/Na^{+}$ cation ratios and on an activated carbon adsorbent derived from Paulownia tomentosa wood.

The data show that Ca–Na-type zeolites possess a much higher adsorption capacity compared to the carbon material. The highest capacity (6.0–6.2 mmol/g) is observed for the Ca5Na3[(AlO2)12(SiO2)12] zeolite, which can be attributed to its higher concentration of divalent calcium cations (Ca2+), generating stronger electrostatic fields and forming stable ion–dipole complexes with $H_2S$ molecules.

The Ca4Na4[(AlO2)12(SiO2)12] zeolite exhibits a slightly lower capacity (5.2–5.4 mmol/g) because part of its active sites are occupied by monovalent Na+ cations. However, both zeolites correspond to Type I(a) isotherms, typical of microporous structures and indicative of a monolayer filling mechanism.

In contrast, the Tomentose adsorbent shows a much lower capacity (3.3–3.5 $mmol \cdot g^{-1}$) and corresponds to a Type I(b)) isotherm, characteristic of meso- and macroporous materials. Adsorption on this material proceeds mainly through weak physisorption governed by van der Waals forces.

Thus, increasing the proportion of Ca2+ in the series Ca4Na4®Ca5Na3 enhances the energetic strength of the active sites, increases H2S polarization, and consequently raises the adsorption capacity. Therefore, the Ca5Na3 zeolite can be regarded as the most efficient microporous adsorbent for the selective removal of hydrogen sulfide under low-pressure and ambient-temperature conditions, while the Tomentose adsorbent is suitable only for preliminary gas purification.

## 4. Conclusion

The adsorption isotherms of hydrogen sulfide ($H_2S$) at 303 K on Ca-Na zeolites and a plant-based Tomentose adsorbent revealed significant differences in sorption behavior. The zeolites $Ca_4Na_4[(AlO_2)_{12}(SiO_2)_{12}]$ and $Ca_5Na_3[(AlO_2)_{12}(SiO_2)_{12}]$ exhibited type I(a) isotherms according to the IUPAC classification, indicating a microporous adsorption mechanism dominated by monolayer filling and strong affinity toward $H_2S$ molecules. The maximum adsorption capacity increased from 5.4 mmol/g for $Ca_4Na_4$ to 5.8 mmol/g for $Ca_5Na_3$, which is attributed to the higher content of divalent $Ca^{2+}$ cations. These cations create stronger electrostatic fields and enhance ion–dipole interactions between the zeolite framework and $H_2S$ molecules. This confirms the critical role of the cationic composition in determining the energy distribution and sorption strength of active sites.

In contrast, the Tomentose adsorbent showed a significantly lower capacity (~3.0 mmol/g) and a smoother isotherm profile, reflecting its mesoporous structure and lack of specific cationic adsorption sites. Adsorption on this material proceeds mainly through weak van der Waals interactions, resulting in less efficient capture of $H_2S$. Overall, the Ca-Na zeolites, particularly $Ca_5Na_3$, demonstrated superior capacity and selectivity, making them promising adsorbents for the deep purification of natural gas, biogas, and industrial gas streams from hydrogen sulfide under mild temperature and low-pressure conditions. The findings highlight that modifying the cationic composition of zeolites is an effective strategy to improve their adsorption activity and thermodynamic stability.

## Transparency:

The authors confirm that the manuscript is an honest, accurate, and transparent account of the study; that no vital features of the study have been omitted; and that any discrepancies from the study as planned have been explained. This study followed all ethical practices during writing.

## Copyright:

© 2025 by the authors. This article is an open-access article distributed under the terms and conditions of the Creative Commons Attribution (CC BY) license (https://creativecommons.org/licenses/by/4.0/).

*Edelweiss Applied Science and Technology*
*ISSN: 2576-8484*
*Vol. 9, No. 11: 429-447, 2025*
*DOI: 10.55214/2576-8484.v9i11.10879*
*© 2025 by the authors; licensee Learning Gate*

## References


[1] L. Y. Hsu and C. P. Huang, "Occurrence and removal of per- and polyfluoroalkyl substances (PFAS) in a full-scale groundwater treatment system," *Environmental Science & Technology*, vol. 53, no. 2, pp. 765–772, 2019.

[2] J. G. Speight, *Natural gas: A basic handbook*. Amsterdam, Netherlands: Elsevier, 2022.

[3] J. Yan *et al.*, "Validation and application of CPFD model in simulating gas-solid flow and combustion of a supercritical CFB boiler with improved inlet boundary conditions," *Fuel Processing Technology*, vol. 208, p. 106512, 2020. https://doi.org/10.1016/j.fuproc.2020.106512

[4] A. L. Kohl and R. B. Nielsen, *Gas purification*, 5th ed. Houston, TX: Gulf Professional Publishing, 1997.

[5] T. J. Bandosz, "Surface chemistry and porosity of activated carbons derived from biomass for gas and vapour adsorption," *Journal of Colloid and Interface Science*, vol. 577, pp. 367–382, 2020.

[6] H. Marsh and F. Rodríguez-Reinoso, *Activated carbon*, 1st ed. Amsterdam, Netherlands: Elsevier Science, 2006.

[7] X. Li, Z. Zhang, Y. Chen, and J. Wang, "Adsorption characteristics of hydrogen sulfide on activated carbon: Effects of pore structure and surface chemistry," *Fuel*, vol. 289, p. 119897, 2021.

[8] M. Seredych and T. J. Bandosz, "Understanding the adsorption of hydrogen sulfide on activated carbons: The role of surface chemistry and porosity," *Carbon*, vol. 145, pp. 620–633, 2019.

[9] J. Yang, Y. Li, L. Chen, Q. Zhang, and H. Wang, "Microwave-assisted preparation of biogenic carbons with enhanced microporosity for hydrogen sulfide adsorption," *Microporous and Mesoporous Materials*, vol. 306, p. 110450, 2020.

[10] D. W. Breck, *Zeolite molecular sieves: Structure, chemistry and use*. New York: John Wiley & Sons, 1974.

[11] C. S. Cundy and P. A. Cox, "The hydrothermal synthesis of zeolites: History and development from the earliest days to the present time," *Chemical Reviews*, vol. 103, no. 3, pp. 663-702, 2003. https://doi.org/10.1021/cr020060i

[12] Y. Qian, J. Li, X. Zhang, S. Wang, and D. Zhao, "Recent advances in the synthesis of zeolite LTA: Mechanisms, green approaches, and binderless strategies," *Chemical Engineering Journal*, vol. 419, p. 129676, 2021.

[13] H. Wang, X. Li, Q. Zhang, and L. Chen, "Cation-exchange effects on pore size and electrostatic field strength in zeolite molecular sieves: Implications for adsorption of polar molecules," *Journal of Physical Chemistry C*, vol. 124, no. 22, pp. 12056–12066, 2020.

[14] A. Corma, "From microporous to mesoporous molecular sieve materials and their use in catalysis," *Chemical Reviews*, vol. 97, no. 6, pp. 2373-2420, 1997. https://doi.org/10.1021/cr960406n

[15] A. Jaskūnas, B. Subačius, and R. Šlinkštienė, "Adsorption of potassium ions on natural zeolite: Kinetic and equilibrium studies," *Chemija*, vol. 26, no. 2, pp. 69–78, 2015. https://doi.org/10.6001/chemija.2015.26.2.1

[16] M. Koxxarov, M. Asfandiyorov, and M. Axmadov, "Isotherm of ammonia adsorption on CaA (M-34) zeolite," presented at the Models and Methods for Increasing the Efficiency of Innovative Research: A Collection of Scientific Works of the International Scientific Conference – Berlin (Part pp. 56–60). Berlin, Germany, 2024.

[17] O. Ergashev *et al.*, "Microcalorimetric study of the change in Gibbs free energy and differential entropy of adsorption of water molecules in Zeolite 3A," *Advanced Journal of Chemistry, Section A*, vol. 9, no. 1, pp. 34-43, 2026. https://doi.org/10.48309/ajca.2026.534085.1880

[18] M. Kokhkharov, F. Rakhmatkarieva, U. Mamadaliev, K. Kholmedov, K. Bakhronov, and A. Ganiev, "Hydrogen sulfide adsorption isotherms in zeolite CaA (M-34)," *Universum: Chemistry and Biology Electronic Scientific Journal*, vol. 11, no. 125, pp. 15–20, 2024. https://doi.org/10.32743/UniChem.2024.125.11.18546

[19] M. Kokhkharov, "Enthalpy and entropy change of methanethiol adsorption in zeolite CaA (M-22)," *Mental Enlightenment Scientific-Methodological Journal*, vol. 5, no. 08, pp. 171-178, 2024. https://doi.org/10.37547/mesmj-V5-I8-22

[20] S. Marian, S. Sivashanmugam, C. J. Brown, and V. Hlavacek, "Adsorption/desorption of water and ethanol on 3A zeolite in near-adiabatic fixed bed," *Industrial & Engineering Chemistry Research*, vol. 48, no. 20, pp. 9247-9260, 2009. https://doi.org/10.1021/ie900446v

[21] W. K. Teo and D. M. Ruthven, "Adsorption of water from aqueous ethanol using 3-. ANG. molecular sieves," *Industrial & Engineering Chemistry Process Design and Development*, vol. 25, no. 1, pp. 17-21, 1986. https://doi.org/10.1021/i200032a003

[22] M. Carmo and J. Gubulin, "Ethanol-water adsorption on commercial 3A zeolites: Kinetic and thermodynamic data," *Brazilian Journal of Chemical Engineering*, vol. 14, no. 3, pp. 217–224, 1997. https://doi.org/10.1590/S0104-66321997000300004

[23] E. Lalik, R. Mirek, J. Rakoczy, and A. Groszek, "Microcalorimetric study of sorption of water and ethanol in zeolites 3A and 5A," *Catalysis Today*, vol. 114, no. 2-3, pp. 242-247, 2006. https://doi.org/10.1016/j.cattod.2006.01.006

[24] M. Kokhkharov, F. Rakhmatkarieva, K. Bakhronov, M. Rakhmatullaeva, I. Absalyamova, and Y. Karimov, "Differential entropy and thermokinetics of ammonia molecule adsorption on CaA zeolite (M-22)," in *E3S Web of Conferences (Vol. 563, p. 01024). EDP Sciences*, 2024.

[25] O. Ergashev *et al.*, "Energy characteristics, adsorption kinetics, and mechanism of triethylamine adsorption on Cs-ZSM-5 zeolite," *Journal of Applied Organometallic Chemistry*, vol. 6, no. 1, pp. 43–52, 2025. https://doi.org/10.48309/JAOC.2026.546865.1334


*Edelweiss Applied Science and Technology*
*ISSN: 2576-8484*
*Vol. 9, No. 11: 429-447, 2025*
*DOI: 10.55214/2576-8484.v9i11.10879*
*© 2025 by the authors; licensee Learning Gate*

[26] K. Bakhronov, O. Ergashev, A. Ganiev, M. Asfandiyorov, M. Ahkmadov, and K. Kholikov, "Isotherm and basic thermodynamic characteristics of ammonia adsorption in CsZSM-5 zeolite," in *AIP Conference Proceedings (Vol. 3045, No. 1, p. 030071). AIP Publishing LLC*, 2024.

[27] O. Ergashev, K. Bakhronov, N. Akhmedova, S. Abdullayeva, S. Khalilov, and K. Kholikov, "Calorimetric study of methanol adsorption in LiZSM-5 and CsZSM-5 zeolites," in *E3S Web of Conferences (Vol. 401, p. 02023). EDP Sciences*, 2023.

[28] K. Bakhronov, O. Ergashev, A. Sultonov, H. Kholmedov, A. Ganiev, and M. Asfandiyorov, "Basic thermodynamic characteristics and isotherm of ammonia adsorption in NaZSM-5 and LiZSM-5 zeolites," in *E3S Web of Conferences (Vol. 401, p. 02025). EDP Sciences*, 2023.

[29] M. Kokharov, U. Axmedov, F. Rakhmatkarieva, and E. Abdurakhmonov, "Investiga-tion of water sorption to Ca5Na3A zeolite at adsorption of micro calorimetric device," *International Journal of Advanced Research in Science, Engineering and Technology*, vol. 5, no. 7, pp. 13939-13944, 2020.

[30] E. B. Abdurakhmonov, F. G. Rakhmatkarieva, and O. K. Ergashev, "Determination of ammonia's adsorption properties in NaLSX zeolite by calorimetric method," *International Journal of Materials and Chemistry*, vol. 10, no. 2, pp. 17–22, 2020.

[31] A. Starke, C. Pasel, C. Bläker, T. Eckardt, J. Zimmermann, and D. Bathen, "Investigation of the adsorption of hydrogen sulfide on faujasite zeolites focusing on the influence of cations," *ACS Omega*, vol. 7, no. 48, pp. 43665-43677, 2022. https://doi.org/10.1021/acsomega.2c04606

[32] A. Starke, C. Pasel, C. Blaeker, T. Eckardt, J. Zimmermann, and D. Bathen, "Impact of Na+ and Ca2+ cations on the adsorption of H2S on binder-free LTA zeolites," *Adsorption Science & Technology*, vol. 2021, p. 5531974, 2021. https://doi.org/10.1155/2021/5531974

[33] T. Yu, Z. Chen, Z. Liu, J. Xu, and Y. Wang, "Review of hydrogen sulfide removal from various industrial gases by zeolites," *Separations*, vol. 9, no. 9, p. 229, 2022. https://doi.org/10.3390/separations9090229

[34] A. G. Georgiadis, N. D. Charisiou, S. Gaber, K. Polychronopoulou, I. V. Yentekakis, and M. A. Goula, "Adsorption of hydrogen sulfide at low temperatures using an industrial molecular sieve: an experimental and theoretical study," *Acs Omega*, vol. 6, no. 23, pp. 14774-14787, 2021. https://doi.org/10.1021/acsomega.0c06157

[35] E. Abdurakhmonov and N. Dekhkanova, "Thermodynamics of hydrogen sulfide adsorption in Zeolite LiX," in *E3S Web of Conferences (Vol. 413, p. 04004). EDP Sciences*, 2023.

*Edelweiss Applied Science and Technology*
*ISSN: 2576-8484*
*Vol. 9, No. 11: 429-447, 2025*
*DOI: 10.55214/2576-8484.v9i11.10879*
*© 2025 by the authors; licensee Learning Gate*